LA-UR- 10-00814

Approved for public release; distribution is unlimited.

Title:	Cross Delay Line Sensor Characterization
Author(s):	Israel J. Owens, ISR-2 Dennis K. Remelius, C-PCS Joe J. Tiee, C-PCS Steven E. Buck, HPC-1 Stephen R. Whittemore, ISR-3 David C. Thompson, C-CDE Robert Shirey, GS-PO
Intended for:	SPIE Journal

Los Alamos
NATIONAL LABORATORY
EST. 1943

Form 836 (7/06)

Cross Delay Line Sensor Characterization

Israel J. Owens*, Dennis K. Remelius, Joe J. Tiee, Steven E. Buck, Stephen R. Whittemore, David C. Thompson and Robert Shirey

Los Alamos National Laboratory, Los Alamos, NM, USA 87545

ABSTRACT

There exists a wealth of information in the scientific literature on the physical properties and device characterization procedures for complementary metal oxide semiconductor (CMOS), charge coupled device (CCD) and avalanche photodiode (APD) format detectors. Numerous papers and books have also treated photocathode operation in the context of photomultiplier tube (PMT) operation for either non imaging applications or limited night vision capability. However, much less information has been reported in the literature about the characterization procedures and properties of photocathode detectors with novel cross delay line (XDL) anode structures. These allow one to detect single photons and create images by recording space and time coordinate (X, Y & T) information. In this paper, we report on the physical characteristics and performance of a cross delay line anode sensor with an enhanced near infrared wavelength response photocathode and high dynamic range micro channel plate (MCP) gain (> 10^6) multiplier stage. Measurement procedures and results including the device dark event rate (DER), pulse height distribution, quantum and electronic device efficiency (QE & DQE) and spatial resolution per effective pixel region in a 25 mm sensor array are presented. The overall knowledge and information obtained from XDL sensor characterization allow us to optimize device performance and assess capability. These device performance properties and capabilities make XDL detectors ideal for remote sensing field applications that require single photon detection, imaging, sub nano-second timing response, high spatial resolution (10's of microns) and large effective image format.

Keywords: Photocathode, micro-channel plate and remote sensing

1. INTRODUCTION

In contrast to many large image format detection schemes, XDL sensors provide narrow time stamp and spatial information for a given point in the 25 mm imaging space. This imaging space is multi dimensional [1], but for this paper we focus on imaging with a pixel format that is constrained to the 2D plane [2]. The ability to accurately isolate the time and spatial information for a single effective pixel requires knowledge of the relevant sensor physics, read-out electronics and data processing software. This paper is based on the characterization of the XDL sensor highlighting the

experimental setup, operating parameters and features that allow suitability for remote sensing applications.

2. SENSOR CHARACTERIZATION

The heart of the experimental setup consists of the photocathode, micro channel plates and XDL anode. Electrons are released from the photocathode [3], and accelerated toward the gain stage z-stack MCPs. The high dynamic range MCPs create an electron charge cloud that strikes a region on the cross delay lines in the anode. A photo of the sensor unit is shown in Fig. [1]. An event position in 2D space is registered by the time delay recorded from overlapping serpentine wire lines (X=X2-X1, Y=Y2-Y1). A photo of the cross delay line sensor anode is shown in Fig. [2]. The sensor QE is measured by comparing the photon rate computed from a calibrated incandescent light source and intensity radiometer current reading to the photo-electron current collected at the top of the micro channel plate.

Figure 1. Near infrared wavelength enhanced S-25 photocathode cross delay line sensor.

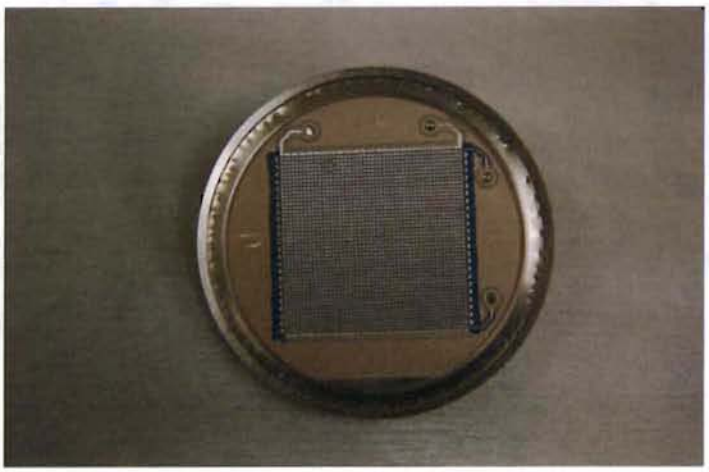

Figure 2. Cross delay line serpentine anode structure.

In order to precisely determine time delays, the four anode signals are sent to a pre-amplifier and processed in a Berkeley Nucleonics DTDC-F module. The propagation and processing of the signals through the electronics modules reduce the measured QE by approximately 60-80% of its nominal value. A plot of the QE and DQE measurements are shown in Fig. [3].

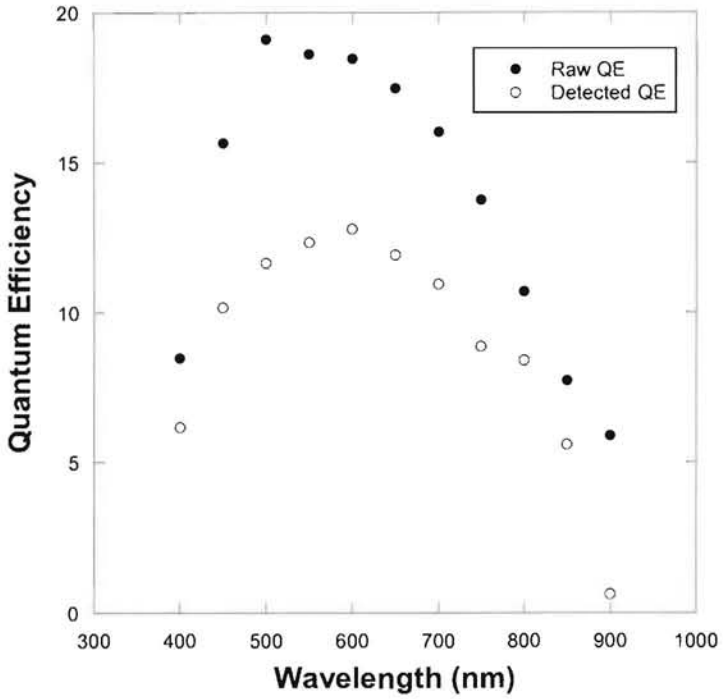

Figure 3. Cross delay line sensor QE and detected QE.

The peak QE and DQE were typically measured at ~ 18-19% and 11-12% for the 500-550 nm spectral range respectively.

This signal timing and effective analog charge values are analyzed in the DTDC-F module and sent for further processing and display in SAO Image DS9 astronomical data visualization application software. This acquisition and imaging software allows us to evaluate properties such as the pulse height distribution and field images in the plane of the sensor. For the pulse height distribution, we record one hundred second files that include the number of counts per second versus arbitrary bins

or channels representing Voltage. A plot of the pulse height distribution measured at a supply of 3700 Volts is shown in Fig. [4].

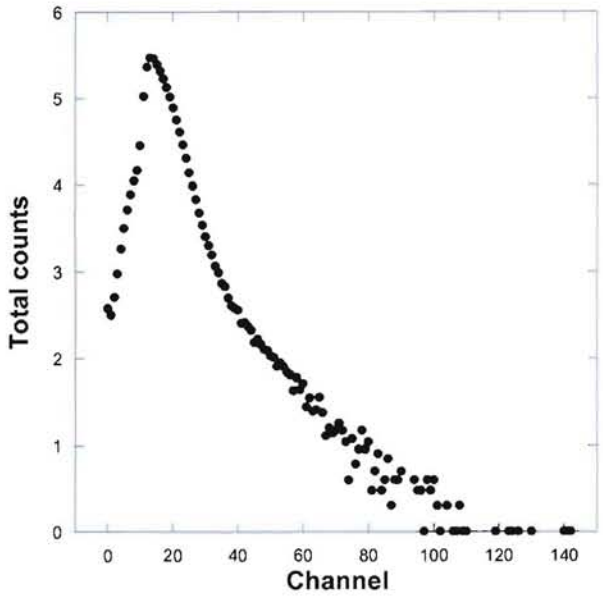

Figure 4. Cross delay line sensor pulse height distribution.

Irregularities in the tail of the distribution provide us with information about the overall device gain and the undesirable presence of physical processes such as ion feedback. However, our tests did not show any unexpected spikes in the distribution that cause or result from ion feedback.

Field images of the 25 mm sensor plane were recorded with and without external light illumination. For the dark field or no light case, we recorded 100 second files and displayed the image and total count rate in DS9 software interface window. Any deviations from field uniformity and the total dark count rate are displayed. The dark count rate was recorded in the range of tens of thousands of

counts per second at ambient operating temperature (21 degrees Celsius) and approximately doubles for every 6 degree Celsius. The dark count rate also can vary up to hundreds of thousands of counts per second depending on irregularities in the manufacturing process that are intended to enhance NIR response.

With the incandescent illumination source turned on, we use a light integrating sphere to approximate a flat field source. Neutral density filters (ND 5-7) are placed in the path of the light to prevent saturation, sensor damage and provide the appropriate illumination level. A picture of the flat field integrating sphere and sensor housing setup is shown in Fig. [5].

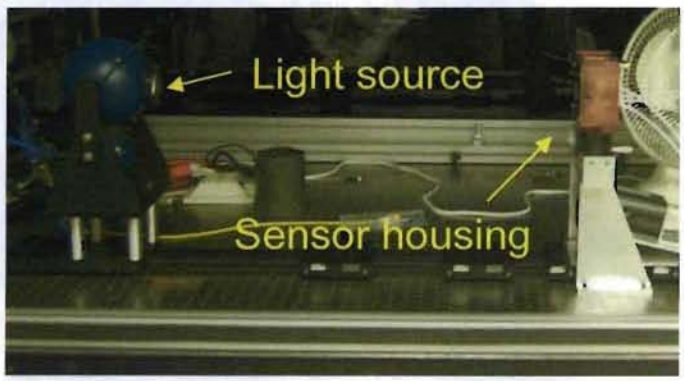

Figure 5. Flat light field integrating sphere and cross delay line sensor housing.

Once a basic check of qualitative plane field images and count rates has been established, we place a focusing lens and pinhole mask in front of the sensor to measure spatial resolution. The lens is positioned on a motor driven Oriel mechanical encoder stage for precise focusing. The pinhole array contains 941 micron spacing between the pinhole center and image plane. A scaling factor is derived from counting the number of pixels between pinhole centers. The overall spatial resolution

can be calculated by multiplying the number of pixels by the nominal scaling factor to obtain length units. A plot of the spatial resolution versus supply Voltage is shown in Fig. [6].

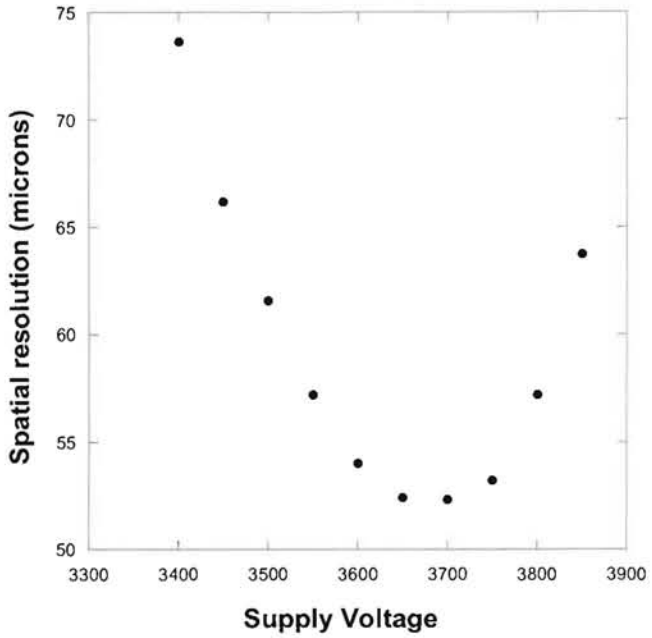

Figure 6. Cross delay line sensor spatial resolution versus supply Voltage.

The optimization of the spatial resolution primarily depends on the quality of the optical focus and the selection of photocathode, MCP and anode. We typically used a total supply Voltage of 3700 with 200 V for the photocathode, 2900 V across the MCP and 600 V applied to the Anode. As shown in the plot, the spatial resolution varied with Voltage from 50-70 microns with the narrowest resolution value of 52 microns at 3700 V.

The sensor timing resolution is 100 ps and characterization measurements are only limited by physical sensor transit time and electronic component jitter. The MCP and anode pulses were

recorded with 2-4 ns rise and fall times. The electronic jitter between the pulse output of the MCP and anode is ~ 11 ns.

3. DISCUSSION AND SUMMARY

In summary, we have considered the physical characterization properties of the XDL sensor. A series of carefully formulated tests revealed the optimal operating parameters for device operation. The QE at visible and enhanced NIR wavelength was shown to be suitable for detecting single photons emitted from a spectrally filtered incandescent light source. The overall spatial resolution was determined to thousands of effective pixel format base on less than 100 micron resolution with sub nano-second timing capability. All characterization results combined demonstrated that the XDL sensor is ideal for applications that require relatively large image format and fast timing response per effective pixel such as remote sensing of terrain and detection of rapidly moving objects [4] and debris.

REFERENCES

[1] Priedhorsky, W.C., Smith, R.C. and Ho, C., "Laser ranging and mapping with a photon-counting detector," Applied Optics, Vol. 35, No. 3, (1996).

[2] Siegmund, O., Vallerga, J., Jelinsky, P., Michalet, X. and Weiss, S., Proc. IEEE Nuclear Science Symposium Conference Record, (2005).

[3] Ahmed, S.N., [Physics & Engineering of Radiation Detection], Academic Press, San Diego, (2007).

[4] Priedhorsky, W.C. and Bloch, J. J., "Optical detection of rapidly moving objects in space," Applied Optics, Vol. 44, No. 3, (2005).